



# Photocatalysis assisted simultaneous carbon oxidation and NO<sub>x</sub> reduction



Lijun Liao<sup>a</sup>, Steven Heylen<sup>a</sup>, Sreeprasanth Pulinthanathu Sree<sup>a</sup>, Brecht Vallaey<sup>a</sup>, Maarten Keulemans<sup>a,b</sup>, Silvia Lenaerts<sup>b</sup>, Maarten B.J. Roeffaers<sup>a</sup>, Johan A. Martens<sup>a,\*</sup>

<sup>a</sup> Centre for Surface Chemistry and Catalysis, KU Leuven, Celestijnenlaan 200F, Bus 2461, 3001 Heverlee, Belgium

<sup>b</sup> Research Group Sustainable Energy and Air Purification, Department of Bioscience Engineering, University of Antwerp, Groenenborgerlaan 171, B-2020 Antwerp, Belgium

## ARTICLE INFO

### Article history:

Received 30 June 2016

Received in revised form

13 September 2016

Accepted 22 September 2016

Available online 23 September 2016

### Keywords:

Titanium dioxide

Photocatalysis

Carbon

Nitrogen oxide

Nitrogen

## ABSTRACT

Photocatalysis assisted oxidation of carbon black was performed using TiO<sub>2</sub> photocatalyst under UV illumination in an atmosphere with NO, O<sub>2</sub> and water vapor at 150 °C. Carbon is oxidized mainly to CO<sub>2</sub> while NO is selectively converted to N<sub>2</sub>. Enhanced O<sub>2</sub> and NO concentrations have a positive effect on the carbon oxidation rate. At a concentration of 3000 ppm NO and 13.3% O<sub>2</sub> in the gas phase the carbon oxidation rate reaches 2.3 μg<sub>carbon</sub>/mg<sub>TiO2</sub> h, at a formal electron/photon quantum efficiency of 0.019. HR SEM images reveal uniform gradual reduction of the carbon particle size irrespective of the distance to TiO<sub>2</sub> photocatalyst particles in the presence of NO, O<sub>2</sub> and H<sub>2</sub>O.

© 2016 Elsevier B.V. All rights reserved.

## 1. Introduction

Controlled oxidation of carbon nanoparticles is of interest to many practical applications. Regeneration of diesel particulate filters is a prominent example. A common filter regeneration strategy involves oxidation of the carbon deposit using NO<sub>2</sub> obtained by catalytic oxidation of NO emitted by the engine [1]. NO<sub>2</sub> mediated carbon oxidation proceeds at temperatures exceeding 250 °C, and NO<sub>2</sub> is reduced mainly to NO rather than N<sub>2</sub>, necessitating an additional DeNO<sub>x</sub> system downstream from the filter [1]. In nanotechnology, oxidative modification of carbon nanomaterials is needed for selective elimination of amorphous carbon debris, and for altering physico-chemical properties such as enhancing hydrophilicity. To this purpose carbon nanotubes (CNTs) are oxidized with concentrated mineral acid (e.g. nitric acid and sulfuric acid) to facilitate dispersion in polar solvents [2,3]. Graphitic oxide obtained by oxidation of graphite with the mixture of strong oxidants (nitric acid, sulfuric acid or potassium permanganate) [4,5]. Improved methods have been reported, concentrated acid and

strong oxidants are necessary for the oxidation process [6,7]. More sustainable chemical methods would be welcome [6].

Photocatalytic oxidation is mentioned among the green chemistry methods for sustainable development [8]. The method has been used to oxidize carbon, and for converting NO<sub>x</sub> to N<sub>2</sub> various ways, and the possibility of combining both reactions has been suggested. Titanium dioxide is widely used for photocatalytic applications for its commercial availability and robustness [8]. UV light is needed for charge separation in TiO<sub>2</sub> semiconductor because of the large band gap of crystalline TiO<sub>2</sub> phases (anatase: 3.2 eV, rutile: 3.03 eV) [9]. Soot can be oxidized using sunlight-driven photocatalysis on TiO<sub>2</sub>. Self-cleaning properties of TiO<sub>2</sub> coatings covered by soot have been demonstrated [10–16]. The efficiency of this photocatalytic process proceeding outdoors is, however, very low [10]. Oxidation of a 0.5 μm soot deposit requires e.g. 45 days [10,17].

NO<sub>x</sub> elimination from air using photocatalysis is an emerging technology. Photocatalytic NO<sub>x</sub> oxidation converts NO with O<sub>2</sub> to NO<sub>2</sub>, which reacts further to nitrates that can be removed from the photocatalyst by water leaching. This deNO<sub>x</sub> concept has been implemented e.g. on the surface of concrete pavement [18,19]. Titanium dioxide which is photoactive under UV light achieves photodecomposition of NO to N<sub>2</sub> and O<sub>2</sub> [8]. The reaction is slow and inhibited by O<sub>2</sub>. Substantial N<sub>2</sub>O by-product formation is observed [20–22]. Modified TiO<sub>2</sub> and zeolites have been investigated to

\* Corresponding author.

E-mail address: [johan.martens@biw.kuleuven.be](mailto:johan.martens@biw.kuleuven.be) (J.A. Martens).

improve catalyst activity and  $N_2$  selectivity of the NO decomposition reaction with some success [23]. Additionally, the photo-SCR activity of commercial and modified  $TiO_2$  in the presence of sacrificial reducing agents such as  $NH_3$ , CO and short-chain hydrocarbon reductants has been demonstrated [24–32]. In nanotechnology, photocatalytic oxidation potentially is a sustainable method for the preparation of a variety of carbon materials such as oxidized carbon nanotubes and graphite oxide.

In a previous publication we reported that carbon black can be selectively photo-oxidized to  $CO_2$  using NO in absence of  $O_2$  [33]. Under those conditions in absence of  $O_2$ , NO was converted to  $N_2$ . The observed carbon oxidation rate was relatively low (ca.  $2 \mu g_{\text{carbon}}/mg_{TiO_2} h$ ). In this paper we investigate the potential of photocatalytic oxidation of carbon using reactive gas mixtures with ppm quantities of NO in addition to  $O_2$ . Promising results were obtained showing enhanced carbon oxidation rates and even oxidation of all carbon particles. Interestingly, NO is selectively reduced to  $N_2$  even in the presence of  $O_2$ . The size reduction of carbon particles up on oxidation is monitored with HR SEM.

## 2. Experimental

### 2.1. Sample preparation

Millennium PC500 (Cristal Global) was used as  $TiO_2$  photocatalyst. This photocatalyst has a high surface area of  $350 m^2/g$  and a primary particle (not aggregates) size of 9 nm [34]. The carbon black material was Printex U (Evonik) considered as a synthetic mimic of soot [35]. An amount of 5 mg of Printex U was deposited on glass plates ( $430 mm \times 70 mm$ ) by spreading a suspension of Printex U in isopropanol. Samples were dried overnight at  $120^\circ C$ . 50 mg of  $TiO_2$  catalyst powder was deposited on the soot coated glass plate from an isopropanol suspension afterwards.

### 2.2. Photocatalytic reaction

The photocatalytic reaction was carried out in a home-made flat photoreactor [33]. The prepared sample was illuminated from the top with a UV lamp (Rayonet) at a light intensity of  $1.1 mW/cm^2$ . Gases were fed from gas cylinders using mass flow controllers (Bronkhorst). More information concerning the experimental setup and the gas analyzers can be found elsewhere [33]. The  $CO$ ,  $CO_2$ ,  $NO_x$  ( $NO$  &  $NO_2$ ) and  $N_2O$  content in the reactor volume are analyzed after the illumination period using UV spectroscopy and NDIR (ABB Limas 11HW and Uras 26 gas analyzers). The photoreactor was operated in batch type experiments as follows. The reactor was purged first under a flow of dry  $N_2$  gas at  $150^\circ C$  for 30 min. Subsequently, the reagent gas mixture was sent through the reactor in absence of light. After reaching the desired  $NO_x$  concentrations (measured using the  $NO_x$  analyser at the outlet), the gas inlet and outlet were closed. At the end of an illumination period, the product gas mixture was conducted to the gas analysers using carrier gas.

### 2.3. Quantification of nitrates

Quantitative determination of nitrates was performed on spent catalysts which were scraped from the glass plate. Nitrates were dissolved by slurring the scraped powder in deionized water. Solids were removed by filtration. Dissolved nitrate was determined using a Hach Lange LCK 339 or 340 test kit. The conversion of NO to  $N_2$  was determined from the N-atom balance over the reactor.

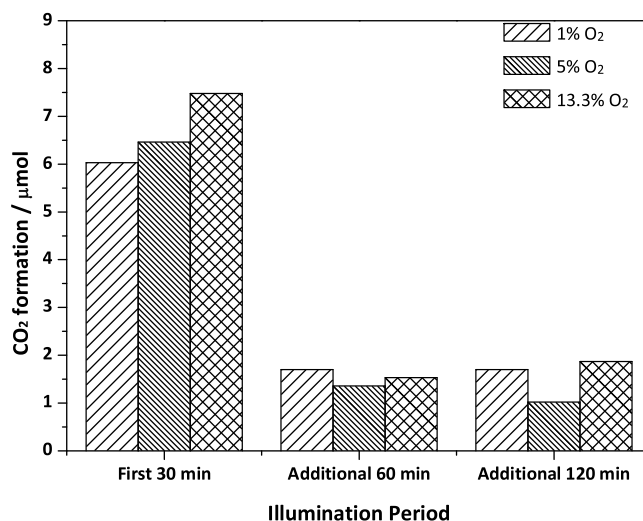


Fig. 1.  $CO_2$  formation in photocatalytic oxidation of carbon black in presence of  $TiO_2$  in a gas mixture with varied  $O_2$  concentration and 3%  $H_2O$ .

### 2.4. Fourier transform infrared (FTIR) measurements

Fourier Transform Infrared (FTIR) spectra of scraped powder diluted in KBr (0.5 mg in 473 mg KBr) were recorded on a Bruker IFS 66 v/s.

### 2.5. High-resolution scanning electron microscopy (HR SEM) measurements

HR SEM images were recorded using low accelerating voltages (2 kV) with a Nova NanoSEM450 (FEI) equipped with BSE detectors, Concentric Backscattered detector (CBS), Through Lens Detector (TLD) combined with a beam deceleration mode (utilizing a stage bias up to 4 kV). The layer of carbon black and  $TiO_2$  was deposited on an aluminium plate and imaged before and after carbon photo-oxidation. SEM images were taken on samples as such without any further modification.

## 3. Results and discussion

Printex U is commonly used as a model carbon material for investigating kinetics of carbon oxidation processes [36]. It is considered to be a good model for the elemental carbon portion of particulate matter emitted by diesel and gasoline direct injection engines [37,38]. A layer of 5 mg carbon black covered by 50 mg  $TiO_2$  was exposed to UV light in a closed flat-plate photoreactor filled with gas mixtures containing 3%  $H_2O$  and  $O_2$  at three different concentrations (1%, 5% and 13.3%). The reaction proceeded very slowly at room temperature and was accelerated upon heating. A reaction temperature of  $150^\circ C$  was selected. The gas composition in the reactor was analyzed after illumination for 30 min. New gas was introduced and illumination continued for 60 min. The procedure was repeated for a third 120 min illumination period. The obtained photocatalytic oxidation of carbon to  $CO_2$  is presented in Fig. 1.  $CO$  was always formed in much smaller quantities than  $CO_2$  (typically only about 2% of the oxidized carbon, see Supporting information). Much more  $CO_2$  was formed in the first illumination period compared to the second and third period. Increasing the  $O_2$  concentration enhanced  $CO_2$  formation especially in the first run. Printex U type carbon black contains a variety of carbon species including easily oxidized oxygenated groups [39]. This carbon fraction is oxidized first [37]. Refractory carbon representing the main share of carbon black is more difficult to oxidize [40–42]. Photocat-

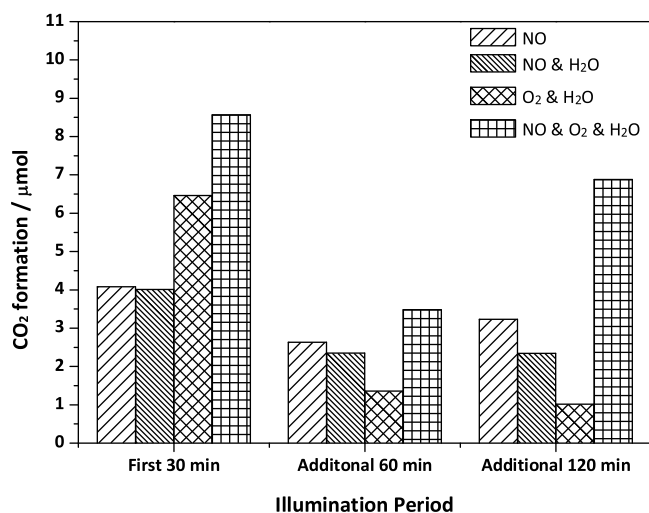


**Fig. 2.** CO<sub>2</sub> formation in photocatalytic oxidation of carbon black in presence of TiO<sub>2</sub> under different atmospheres. Concentrations: NO: 3000 ppm, O<sub>2</sub>: 5%, H<sub>2</sub>O: 3%. Fresh gas mixture introduced in the photoreactor before additional illuminations. The results in the presence of NO alone and of NO & H<sub>2</sub>O were taken from previous publication for comparison [33].

alytic oxidation of the refractory carbon using O<sub>2</sub> and water only is slow. Under these reaction conditions, carbon oxidation probably proceeds via reaction with hydroxyl radicals (OH•) and superoxide anions (O<sub>2</sub><sup>-</sup>) formed from adsorbed water and molecular oxygen, respectively [11–15].

The composition of the gas atmosphere was altered in subsequent experiments and the influence of oxygen and water concentration studied (Fig. 2). With 3000 ppm NO in the gas phase without water and O<sub>2</sub>, ca. 4.1 μmol CO<sub>2</sub> was formed in the first period. Replacing the gas and continuing illumination produced an additional 2.6 μmol of CO<sub>2</sub> a first time, and 3.2 μmol a second time. Adding 3% water to NO had no influence initially and decreased CO<sub>2</sub> formation in the second and third period (Fig. 2). In an atmosphere with 5% O<sub>2</sub> and water initially more CO<sub>2</sub> was formed (6.46 μmol). In the second and third illumination period little CO<sub>2</sub> was formed, viz. 1.36 μmol and 1.02 μmol (data from Fig. 1 added to Fig. 2), substantially less than with NO with and without water. Carbon oxidation went best in presence of both NO and O<sub>2</sub> (Fig. 2). In the first period 8.57 μmol CO<sub>2</sub> was formed, and 3.48 μmol and 6.88 μmol in the second and third period, respectively.

From this series of experiments it can be concluded that the first illumination period dealing with easily oxidized carbon of the carbon black material is most CO<sub>2</sub> productive, independent of gas composition which is in accordance with literature [37]. NO in the gas phase is essential to enhance CO<sub>2</sub> formation later in the reaction when refractory carbon is oxidized.

A key question is whether there is a synergetic effect of NO and O<sub>2</sub> in photocatalytic carbon oxidation. In the first period the formation of CO<sub>2</sub> in presence of both NO and O<sub>2</sub> amounted to 8.57 μmol, which is lower than the sum of CO<sub>2</sub> formed in presence of NO (4.1 μmol) and O<sub>2</sub> (6.5 μmol), suggesting competition rather than synergism. In the second run, there was no synergy either. Only in the third period combination of NO and O<sub>2</sub> generated an amount of CO<sub>2</sub> (6.88 μmol) exceeding the amount obtained with the two gases separately (3.22 μmol and 1.02 μmol, Fig. 2). This observation suggests that O<sub>2</sub> and NO compete initially for oxidation of the easily oxidized carbon, while they cooperate later on in the oxidation of the refractory carbon. Compared to the results in absence of oxygen, both oxygen and nitrogen monoxide have a positive effect on the amount of CO<sub>2</sub> formed.

**Table 1**  
NO conversion and selectivity in carbon photooxidation.

Reaction	NO <sub>x</sub> conversion (%)	Selectivity (%)			NO <sub>3</sub> <sup>-</sup> (μg) <sup>a</sup>
		N <sub>2</sub>	N <sub>2</sub> O	NO <sub>3</sub> <sup>-</sup>	
First 30 min	99	78	11	11	1
Additional 60 min	99	80	1	19	2.6
Additional 120 min	97	99	1	0	2.4

Gas composition: 3000 ppm NO, 5% O<sub>2</sub>, 3% H<sub>2</sub>O.

<sup>a</sup> Determined on scraped layer after reaction.

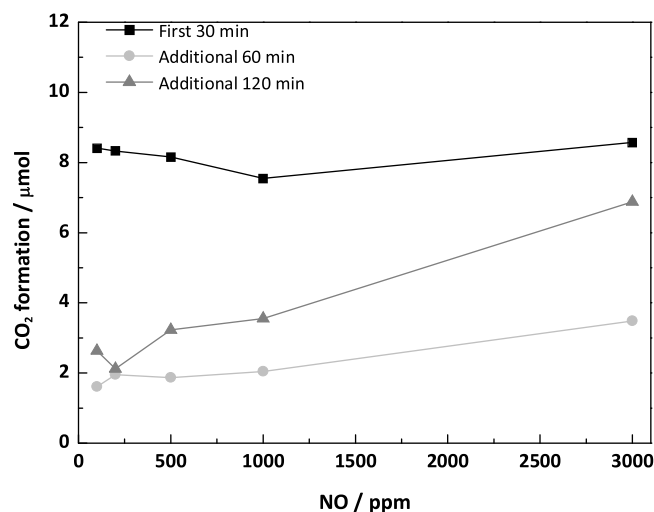


**Fig. 3.** CO<sub>2</sub> formation by photocatalytic oxidation of carbon black in the presence of TiO<sub>2</sub> in the presence of gas mixture with varied NO concentration and fixed concentrations of O<sub>2</sub> (5%) and water vapor (3%).

The obtained levels of NO conversion and the selectivity are reported in Table 1. After 30 min illumination of a fresh soot – TiO<sub>2</sub> layer in contact with gas mixture containing 3000 ppm NO, 5% O<sub>2</sub> and 3% water. NO<sub>x</sub> in the headspace of the reactor was converted for 99%, with 78% N<sub>2</sub> selectivity, 11% N<sub>2</sub>O and 11% nitrate (determined on scraped layer). The experiment was repeated on a new layer of soot and TiO<sub>2</sub>. After 30 min illumination, the reactive gas was evacuated and new gas mixture introduced. After another 60 min illumination, the gas phase was analysed. 99% NO<sub>x</sub> conversion was reached, with 80% N<sub>2</sub> selectivity, 1% N<sub>2</sub>O and 19% nitrate. Finally, another fresh layer of soot and TiO<sub>2</sub> was loaded in the photoreactor, and subjected to the 30 and 60 min illumination procedure. A third illumination for 120 min resulted in 97% NO<sub>x</sub> conversion, with 99% N<sub>2</sub> selectivity. The final nitrate content was 2.4 μg, similar to the content after 60 min. Apparently, no additional nitrate was deposited during the third illumination period.

The synergetic effect between NO and O<sub>2</sub> was further explored with an experiment in which the NO concentration in the gas mixture was varied while keeping the O<sub>2</sub> (and H<sub>2</sub>O) concentration constant (Fig. 3). CO<sub>2</sub> formation in the first illumination period was rather insensitive to NO concentration, while in the second and especially in the third illumination periods, handling the more difficult to oxidize carbon, CO<sub>2</sub> formation increased with increasing NO content of the gas mixture. The tendency that more CO<sub>2</sub> is formed in the third illumination compared to the second initially observed at 3000 ppm (Fig. 3) is also observed at lower NO concentrations (Fig. 3). The longer duration of the third period (120 min) compared to the second one (60 min) may explain this difference. As mentioned previously, this carbon material contains easy to oxidize and hard to oxidize carbon. Therefore part of the carbon material were oxidized first at a relatively high carbon oxidation rate (in the first 30 min reaction in the presence of either oxygen or NO, Fig. 2).

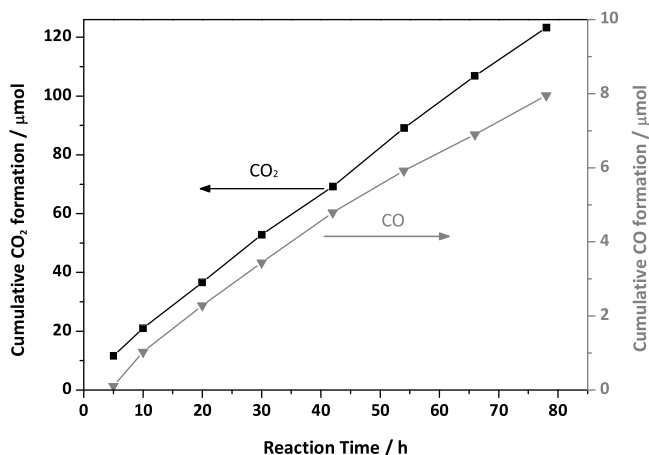


**Fig. 4.** Cumulative CO<sub>2</sub> and CO formation during a long carbon photo-oxidation experiment in the presence of NO, O<sub>2</sub> and H<sub>2</sub>O. Gas composition; 3000 ppm NO, 3% H<sub>2</sub>O, 5% O<sub>2</sub>.

At this reaction stage, the carbon oxidation rate apparently cannot be increased by increasing the NO concentrations. In subsequent illumination periods, the remaining part of refractory carbon material is oxidized at a lower carbon oxidation rate. NO and O<sub>2</sub> have a synergetic effect on the oxidation of this type of carbon material, as shown in Fig. 2. Thus the carbon oxidation rate was effectively increased by increasing the NO concentrations in the third, 120 min illumination period.

In these experiments, in each illumination period NO was almost entirely converted. N<sub>2</sub>O was formed especially in the first and second illumination periods in values similar to the values reported in Table 1. High selectivity to N<sub>2</sub> was obtained in the second and especially in the third illumination period.

The highest carbon oxidation rate of ca. 5.64 μg carbon per hour per mg TiO<sub>2</sub> was obtained in the experiment with 3000 ppm NO, 13.3% O<sub>2</sub> and 3% H<sub>2</sub>O at 150 °C during the first 30 min for the easily oxidized carbon. For the refractory carbon an oxidation rate of 2.27 μg carbon per hour per mg TiO<sub>2</sub> was obtained in the third illumination period. Such reaction rate is rather low compared to thermal catalysis at higher temperatures (300–500 °C) (see Supporting information). The incident light intensity of the reactive layer in the photoreactor is about  $2.9 \times 10^{17}$  photons s<sup>-1</sup>. An electron/photon formal quantum efficiency of 0.019 can be estimated from the formal quantum efficiency assuming carbon oxidation to be a 4-electron redox reaction. This value is higher than the reported photocatalytic oxidation of burning ‘T-lite’ soot on TiO<sub>2</sub> coating under UV irradiation in air ( $4.4 \times 10^{-4}$ ) [10].

A long experiment was performed with 78 h of continuous illumination (Fig. 4). Eight consecutive reactions were performed with UV exposure times ranging from 5 to 12 h, each time with a fresh gas mixture with 3000 ppm NO, 5% O<sub>2</sub> and 3% H<sub>2</sub>O contacting the same soot-TiO<sub>2</sub> layer. In total 123.3 μmol CO<sub>2</sub> together with 7.9 μmol CO was formed (Fig. 4), corresponding to oxidation of about 30% of carbon loaded in the photoreactor. The carbon oxidation rate remained rather stable over this 78 h period.

The NO<sub>x</sub> conversion was ca. 99% in each of the eight runs. Some N<sub>2</sub>O was formed only in the first illumination (3%). In second and later illuminations N<sub>2</sub> was the only detected N-containing gaseous reaction product. The final nitrate content of the layer was 3.2 μmol and only slightly higher compared to the results obtained for shorter reaction times (Table 1).

The presence of nitrate on the samples after photocatalysis was confirmed with FTIR (Fig. 5). On a UV-illuminated layer of TiO<sub>2</sub> (without carbon) exposed to the reactive gas mixture a sharp absorption band at 1386 cm<sup>-1</sup> was observed (Fig. 5a). This sig-

nal was assigned to nitrate on the surface of TiO<sub>2</sub> photocatalyst [43]. The broad band around 3410 cm<sup>-1</sup> and the peak around 1635 cm<sup>-1</sup> were assigned to the stretching and bending vibrations of physisorbed water [15,44]. The broad peak centred at 530 cm<sup>-1</sup> was ascribed to bending of Ti-O bonds [45]. A layer of soot and TiO<sub>2</sub> exposed 78 h to UV light under reactive gas mixture showed a similar FTIR spectrum (Fig. 5b). In addition to these signals, a layer containing both soot and TiO<sub>2</sub> after reaction shows distinct IR absorption signatures that can be attributed to partially oxidized carbon. For instance in the spectrum of soot and TiO<sub>2</sub> subjected to three runs (Fig. 5d), absorption at 1260 cm<sup>-1</sup> can be attributed to the C–O–C stretching in an anhydride or aryl ether linkage [46]. The signal around 1100 cm<sup>-1</sup> can be assigned to C–C and C–H plane deformation of aromatic groups [47]. The band at 800 cm<sup>-1</sup> could be ascribed to the C–H out-of-plane bending of highly substituted aromatic compounds [46]. The small peak at 2918 cm<sup>-1</sup> is due to the C–H asymmetric stretching vibrations [46].

Under UV illumination, nitrate is formed on the TiO<sub>2</sub> surface from the reaction of nitric oxide with photo-generated hydroxyl radicals [48]. NO<sub>2</sub> is formed as an intermediate which could be further oxidized into nitrate by •OH radicals. However, the formed nitrates can be consumed by the reaction of HNO<sub>3</sub>/NO<sub>3</sub><sup>-</sup> with NO in the presence of TiO<sub>2</sub>. Therefore, formation and decomposition of nitrate on TiO<sub>2</sub> is a dynamic process and steady-state concentration in the layer reflects the dynamic equilibrium of nitric acid formation and transfer to the carbon surface via the gas phase. The N<sub>2</sub>O formation on fresh TiO<sub>2</sub> has been explained by reaction of NO on photo-generated Ti<sup>3+</sup> centers. When the TiO<sub>2</sub> surface is covered by nitrate less of these sites are available, which could explain why N<sub>2</sub>O formation is suppressant in second and third illumination periods.

Size reduction of the carbon black particles during photocatalysis assisted oxidation was investigated with HR SEM (Figs. 6 and 7). To this purpose TiO<sub>2</sub> and carbon were deposited on aluminum support for SEM and treated in the photoreactor. The large white aggregates on the SEM pictures are TiO<sub>2</sub> particles. The small grey spheres are carbon particles. The initial size of original carbon black particles (not aggregates) measure  $45 \pm 7$  nm. With progression of the photocatalysis assisted oxidation, changes of the carbon particle size were observed. After 10 h reaction in the presence of 5% O<sub>2</sub> and 3% H<sub>2</sub>O, some of the carbon particles near TiO<sub>2</sub> photocatalyst were reduced in size (Fig. 6). After 24 h reaction, most of the carbon particles in the vicinity of TiO<sub>2</sub> were even more reduced in size and in some areas, carbon particles were no longer present (Fig. 6). Carbon particles at longer distance from TiO<sub>2</sub> aggregates retained their original size. In photocatalytic oxidation reactions on TiO<sub>2</sub> it is well known the substrate does not need to be adsorbed on the TiO<sub>2</sub> surface. Remote or lateral photocatalytic oxidation of organic substrate has been reported. For instance, remote bleaching of dyes and oxidation of organic compounds was observed in a photoreactor in which TiO<sub>2</sub> and dye were coated on opposing surfaces separated by a small gap (12–50 μm) [49,50]. Oxygen-containing functional groups were introduced in polystyrene by the remote oxidation in such photoreactor [50]. In another experiment, soot deposited alongside TiO<sub>2</sub> film was oxidized preferentially and the gap distance between the soot and TiO<sub>2</sub> increases with the irradiation time [14]. This lateral oxidation process was attributed to the migration of the photo-generated oxidizing species toward the carbon particles.

Remote soot oxidation was also observed with ‘‘T-lite’’ candle soot layer spaced by 175 μm from a TiO<sub>2</sub> coating [11]. Oxidation of soot was observed in the area where the soot was opposing the TiO<sub>2</sub> coating and progressed very slowly further away from TiO<sub>2</sub>. A similar observation was made in this work. Carbon particles at distances of ca. 3 μm from TiO<sub>2</sub> remained intact.



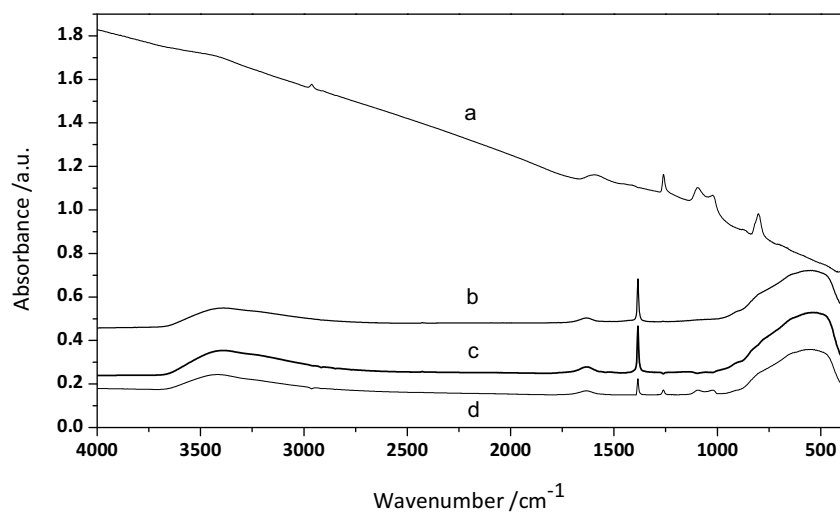


**Fig. 5.** FTIR spectra of scraped powder from the support glass: (a) carbon black before reaction; (b) nitrate-saturated TiO<sub>2</sub> photocatalyst layer (without carbon) after 3 h exposure to a gas mixture with 3000 ppm NO, 5% O<sub>2</sub> and 3% H<sub>2</sub>O (30 ml/min) under UV light at 150 °C; (c) carbon black – TiO<sub>2</sub> layer after 8 consecutive reactions (total reaction time of 78 h); (d) carbon black – TiO<sub>2</sub> layer after three consecutive NO<sub>x</sub> reductions (experiment of Table 1).

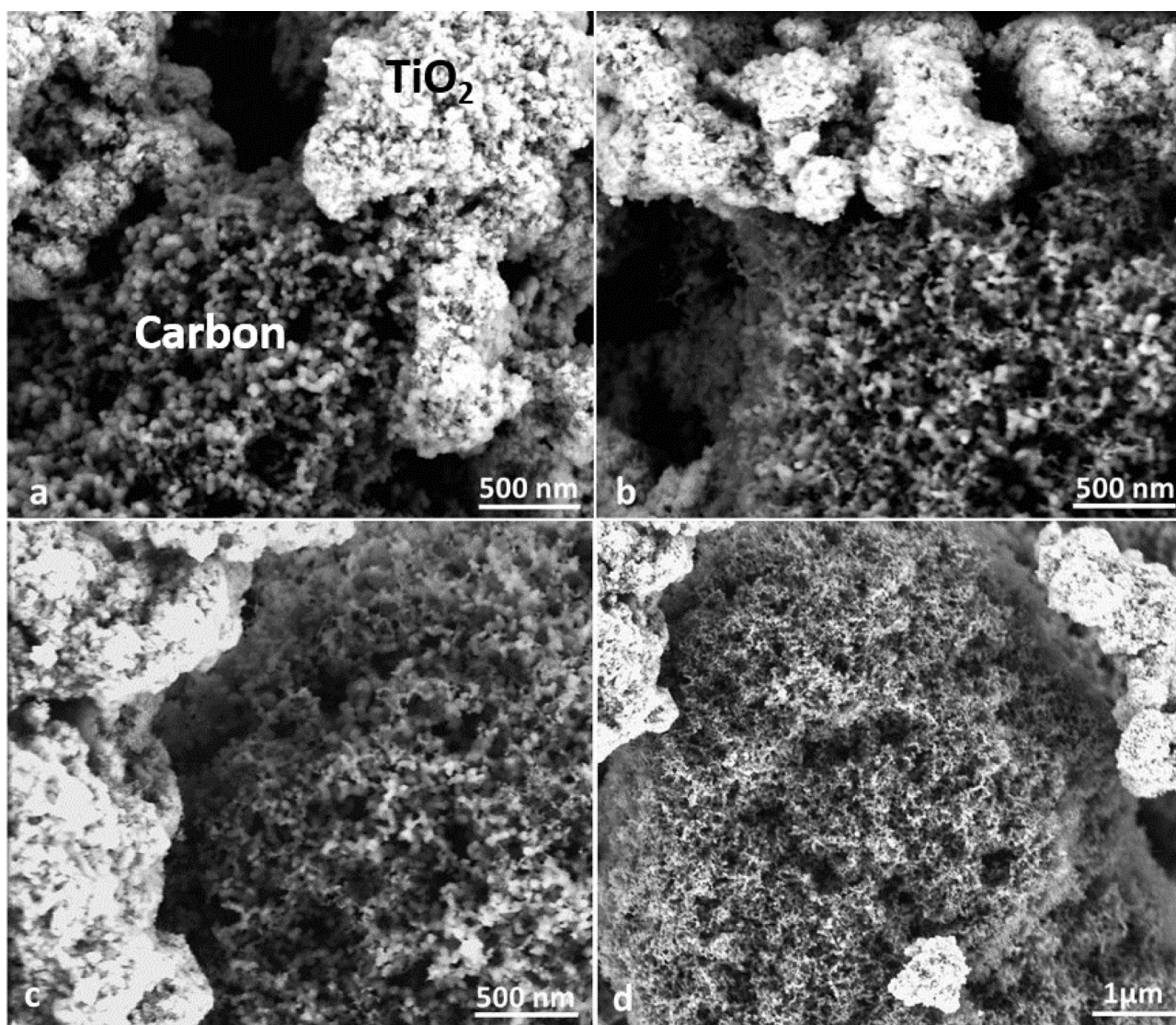


**Fig. 6.** HR SEM images of samples deposited on aluminium plate. (a): before reaction; (b): after 10 h UV irradiation; (c) and (d): after 24 h UV irradiation under an atmosphere with 5% O<sub>2</sub> and 3% H<sub>2</sub>O at 150 °C. White aggregates = TiO<sub>2</sub>; small grey spheres = carbon particles.

A different picture emerged when photocatalytic carbon oxidation was performed in presence of NO and O<sub>2</sub> (Fig. 7). The size of the carbon particles was uniformly reduced. After 10 h continuous exposure to UV light in the presence of reactive gas mixture, the carbon particle size was reduced to  $28 \pm 7$  nm. After 24 h of reaction the carbon particle diameter was further reduced to  $17 \pm 4$  nm. General inspection of the sample with HR SEM revealed homogeneous carbon particle size reduction, a gradual fining of the carbon particle network was observed independent of the distance to TiO<sub>2</sub> particles. Apparently, contact between carbon and TiO<sub>2</sub> is not needed for achieving carbon oxidation and gaseous reaction intermediates must be involved spreading better than in absence of NO<sub>x</sub>. Oxidizing species generated in the presence of nitric oxide, oxygen and water are postulated to be migrating over longer distances to reach the carbon surface than in the absence of nitric oxide. This hypothesis is based on the CO<sub>2</sub> formation data (Fig. 2) and the HR SEM observations (Figs. 6 and 7) which were obtained in the experiments in the presence or absence of NO. In the presence of NO (Fig. 2), more CO<sub>2</sub> was formed especially in the second and third illumination periods than in the experiments in absence of NO. This means the gas mixture with NO can oxidize more carbon particles than the experiments only with oxygen and water. From the HR-SEM pictures (Fig. 6, after reaction in the presence of O<sub>2</sub> and H<sub>2</sub>O) it could be evident that, in absence of NO, carbon particles close to TiO<sub>2</sub> were more oxidized than distant carbon particles, and the carbon particles at distances of ca. 3 μm from TiO<sub>2</sub> remained intact after reaction. From the HR SEM pictures (Fig. 7, in the presence of NO, O<sub>2</sub> and H<sub>2</sub>O) it is seen that, in the presence of NO, carbon particles close to or far from TiO<sub>2</sub> were uniformly reduced in size after reaction. In the presence of oxygen and water, the photo-generated hydroxyl radicals and oxygen related radicals are assumed to be the oxidizing species for carbon photo-oxidation. In the presence of NO, O<sub>2</sub> and H<sub>2</sub>O, besides the hydroxyl radicals and the oxygen related radicals, nitrogen containing species could also be oxidizing agents. From these observations we postulate that the oxidizing species formed in the presence of NO can migrate longer distance than hydroxyl radicals and oxygen related radicals which are formed in the presence of water and oxygen (without NO). These air-borne or surface-mobile species may be nitrogen containing species such as nitric acid or nitrous acid. Further investigation is needed to identify this species.

A potential use of simultaneous carbon oxidation into CO<sub>2</sub> and NO<sub>x</sub> reduction to N<sub>2</sub> obviously is exhaust gas purification. Currently, particulate matter is removed via a particulate filter, while NO<sub>x</sub> is reduced to N<sub>2</sub> via a NO<sub>x</sub> storage and reduction catalyst or via selective catalytic reduction (SCR). Photo-SCR of NO<sub>x</sub> using NH<sub>3</sub> (Photo-NH<sub>3</sub>-SCR) reductant has been demonstrated [51]. Here we present Photo-C-SCR, i.e. the photocatalysis assisted reduction of NO<sub>x</sub> to N<sub>2</sub> using carbon as reductant. Simultaneous removal of NO<sub>x</sub> and PM at low temperature is very attractive. The obtained carbon oxidation rates are only a small fraction of current state-of-the-art thermal carbon oxidation catalysts at 300–500 °C (carbon oxidation rates using thermal catalysis from literature are provided in Supporting information).

This work suggests that oxidative modification of carbon nanomaterial may also be achieved using photocatalysis. Carbon black is a synthetic nanopowder of elementary carbon produced in large tonnage for use as a pigment and as a filler material to improve heat and electric conductivity, UV light absorption and mechanical properties [36,52,53]. Controlled size reduction using photocatalysis has been achieved (Fig. 7). Carbon nanotubes (CNTs) are often chemically modified via the oxidation with nitric acid to increase their dispersability in water, methanol, or other polar solvents [54]. Treatment of CNTs with boiling nitric acid for 16–48 h is a common procedure [55,56]. Over 60% of the CNTs can be lost after the treatment [2]. Similarly, graphite oxide is generally obtained by

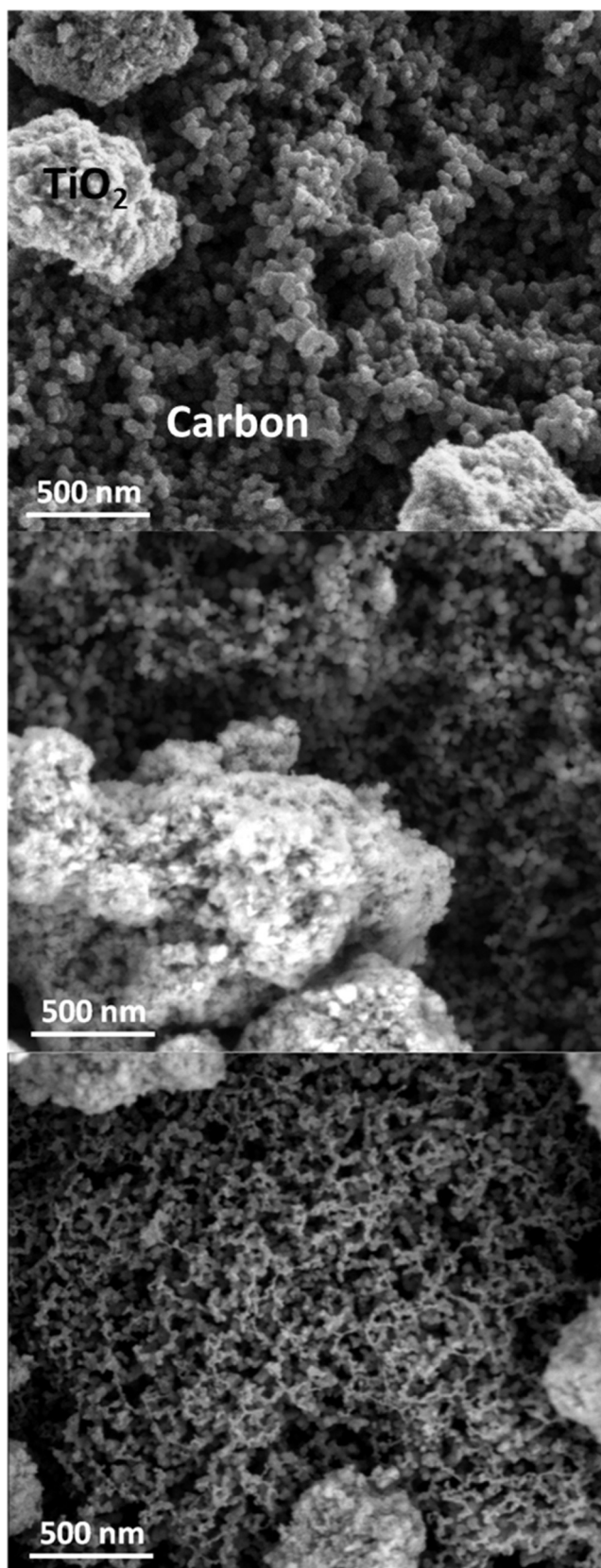


**Fig. 7.** HR SEM images of samples deposited on aluminium plate (taken at same magnification). Upper: before reaction, Middle: after 10 h UV irradiation, Under: after 24 h UV irradiation under an atmosphere with 3000 ppm NO, 5% O<sub>2</sub> and 3% H<sub>2</sub>O at 150 °C. White aggregates = TiO<sub>2</sub>; small grey spheres = carbon particles.



treating graphite with strong oxidants such as in Hummers' method using a mixture of sulfuric oxide, sodium nitrate, and potassium permanganate to oxidize graphite [5]. Formation of gaseous ( $\text{NO}_x$ ) and aqueous waste streams render the method hazardous and unsustainable [6]. Here we have shown oxidation of carbon nano-materials can be achieved by photocatalysis under mild reaction conditions limiting the use of hazardous chemicals and byproduct formation. The potential of this method needs further investigation.

#### 4. Conclusions

Commercial  $\text{TiO}_2$  (Cristal Global PC500) is active in photocatalysis-assisted oxidation of carbon black with nitric oxide and oxygen in the presence of water vapor at  $150^\circ\text{C}$ . Carbon is selectively converted into  $\text{CO}_2$  while  $\text{NO}_x$  is reduced to  $\text{N}_2$ . Up to 30% of the carbon was oxidized without catalyst deactivation. Uniform size reduction of the carbon particles in the presence of  $\text{NO}$ ,  $\text{O}_2$  and  $\text{H}_2\text{O}$  was observed with HR SEM, irrespective of the distance to  $\text{TiO}_2$  photocatalytic particles suggesting the involvement of mobile oxidative species.

Photocatalysis assisted carbon oxidation and  $\text{NO}_x$  reduction may find application in exhaust gas purification. The reduction of  $\text{NO}_x$  selectively to  $\text{N}_2$  using carbon is a new type of SCR catalysis, coined Photo-C-SCR. The highest observed carbon oxidation rate of  $5.64 \mu\text{g}$  carbon per hour per mg  $\text{TiO}_2$  is much below carbon oxidation rates obtained with thermal catalysts in the temperature range  $300\text{--}500^\circ\text{C}$ . At low temperature where thermal catalysts are inactive, photocatalysis may be relevant provided activity is further enhanced.

Photocatalysis assisted oxidation may be an alternative method for modification of carbon nanoparticles. But more work is needed to explore this idea.

#### Acknowledgments

This work was supported by long-term structural funding by the Flemish government (Methusalem). M. Keulemans acknowledges the agency for Innovation by Science and Technology in Flanders (IWT) for financial support (PhD. Grant). M. Roefiaers thanks the ERC for financial support (ERC Starting Grant No. 307523).

#### Appendix A. Supplementary data

Supplementary data associated with this article can be found, in the online version, at <http://dx.doi.org/10.1016/j.apcatb.2016.09.042>.

#### References

- [1] M.V. Twigg, *Catal. Today* 163 (2011) 33–41.
- [2] D. Rosca, F. Watari, M. Uo, T. Akasaka, *Carbon* 43 (2005) 3124–3131.
- [3] V. Datsyuk, M. Kalyva, K. Papagelis, J. Parthenios, D. Tasis, A. Siokou, I. Kallitsis, C. Galiotis, *Carbon* 46 (2008) 833–840.
- [4] B.C. Brodie, *Phil. Trans. R. Soc. Lond.* 149 (1859) 249–259.
- [5] W.S. Hummers Jr., R.E. Offeman, *J. Am. Chem. Soc.* 80 (1958) 1339.
- [6] J. Chen, B. Yao, C. Li, G. Shi, *Carbon* 64 (2013) 225–229.
- [7] D.V. Kosynkin, A.L. Higginbotham, A. Sinitskii, J.R. Lomeda, A. Dimiev, B.K. Price, J.M. Tour, *Nature* 458 (2009) 872–877.
- [8] J. Schneider, M. Matsuoka, M. Takeuchi, J. Zhang, Y. Horiuchi, M. Anpo, D.W. Bahnemann, *Chem. Rev.* 114 (2014) 9919–9986.
- [9] D.O. Scanlon, C.W. Dunnill, J. Buckridge, S.A. Shevlin, A.J. Logsdail, S.M. Woodley, C.R.A. Catlow, M.J. Powell, R.G. Palgrave, I.P. Parkin, G.W. Watson, T.W. Keal, P. Sherwood, A. Walsh, A.A. Sokol, *Nat. Mater.* 12 (2013) 798–801.
- [10] A. Mills, J. Wang, M. Crow, *Chemosphere* 64 (2006) 1032–1035.
- [11] S. Lee, S. McIntyre, A. Mills, *J. Photochem. Photobiol. A* 162 (2004) 203–206.
- [12] M. Smits, C. Chan, T. Tytgat, B. Craeye, N. Costarramone, S. Lacombe, S. Lenaerts, *Chem. Eng. J.* 222 (2013) 411–418.
- [13] T. Tatsuma, S. Tachibana, A. Fujishima, *J. Phys. Chem. B* 105 (2001) 6987–6992.
- [14] M.C. Lee, W. Choi, *J. Phys. Chem. B* 106 (2002) 11818–11822.
- [15] M. Smits, Y. Ling, S. Lenaerts, S. Van Doorslaer, *Chem. Phys. Chem.* 13 (2012) 4251–4257.
- [16] D. Ollis, *Appl. Catal. B* 99 (2010) 478–484.
- [17] T. Boger, D. Rose, P. Nicolin, N. Gunasekaran, T. Glasson, *Emiss. Control Sci. Technol.* 1 (2015) 49–63.
- [18] M.M. Ballari, M. Hunger, G. Husken, H.J.H. Brouwers, *Appl. Catal. B* 95 (2010) 245–254.
- [19] J.K. Sikkema, S.K. Ong, J.E. Alleman, *Constr. Build. Mater.* 100 (2015) 305–314.
- [20] T.H. Lim, S.M. Jeong, S.D. Kim, J. Gyeon, *J. Photochem. Photobiol. A* 134 (2000) 209–217.
- [21] J. Zhang, T. Ayusawa, M. Minagawa, K. Kinugawa, H. Yamashita, M. Matsuoka, M. Anpo, *J. Catal.* 198 (2001) 1–8.
- [22] Y. Hu, G. Martra, J. Zhang, S. Higashimoto, S. Coluccia, M. Anpo, *J. Phys. Chem. B* 110 (2006) 1680–1685.
- [23] J. Lasek, Y.H. Yu, J.C.S. Wu, *J. Photochem. Photobiol. C* 14 (2013) 29–52.
- [24] S. Yamazoe, Y. Masutani, K. Teramura, Y. Hitomi, T. Shishido, T. Tanaka, *Appl. Catal. B* 83 (2008) 123–130.
- [25] K. Teramura, T. Tanaka, T. Funabiki, *Langmuir* 19 (2003) 1209–1214.
- [26] S. Yamazoe, Y. Masutani, T. Shishido, T. Tanaka, *Res. Chem. Intermed.* 34 (2008) 487–494.
- [27] R. Jin, Z. Wu, Y. Liu, B. Jiang, H. Wang, *J. Hazard. Mater.* 161 (2009) 42–48.
- [28] K. Teramura, T. Tanaka, T. Funabiki, *Chem. Lett.* 32 (2003) 1184–1185.
- [29] K. Teramura, T. Tanaka, S. Yamazoe, K. Arakaki, T. Funabiki, *Appl. Catal. B* 53 (2004) 29–36.
- [30] S. Poulston, M.V. Twigg, A.P. Walker, *Appl. Catal. B* 89 (2009) 335–341.
- [31] N. Bowering, G.S. Walker, P.G. Harrison, *Appl. Catal. B* 62 (2006) 208–216.
- [32] A. Yamamoto, K. Teramura, S. Hosokawa, T. Tanaka, *Sci. Technol. Adv. Mater.* 16 (2015) 1–9.
- [33] L. Liao, S. Heylen, B. Vallaey, M. Keulemans, S. Lenaerts, M.B.J. Roefiaers, J.A. Martens, *Appl. Catal. B* 166–167 (2015) 374–380.
- [34] S.M. Verbruggen, K. Masschaele, E. Moortgat, T.E. Korany, B. Hauchecorne, J.A. Martens, S. Lenaerts, *Catal. Sci. Technol.* 2 (2012) 2311–2318.
- [35] N. Nejar, M. Makkee, M.J. Illán-Gómez, *Appl. Catal. B* 75 (2007) 11–16.
- [36] P. Carlsson, *J. Phys. Chem. C* 116 (2012) 9063–9071.
- [37] J.P.A. Neef, T.X. Nijhuis, E. Smakman, M. Makkee, J.A. Moulijn, *Fuel* 76 (1997) 1129–1136.
- [38] A. Setiabudi, M. Makkee, J.A. Moulijn, *Appl. Catal. B* 50 (2004) 185–194.
- [39] H. Muckenhuber, H. Grothe, *Carbon* 44 (2006) 546–559.
- [40] H. An, P.J. McGinn, *Appl. Catal. B* 62 (2006) 46–56.
- [41] B. Frank, M.E. Schuster, R. Schlögl, D.S. Su, *Angew. Chem. Int. Ed.* 52 (2013) 2673–2677.
- [42] R. Niessner, *Angew. Chem. Int. Ed.* 53 (2014) 12366–12379.
- [43] S.K. Srinivasan, S. Ganguly, *Catal. Lett.* 10 (1991) 279–288.
- [44] D.A. Panayotov, J.T. Yates Jr., *Chem. Phys. Lett.* 410 (2005) 11–17.
- [45] Y. Gao, Y. Masuda, Z. Peng, T. Yonezawa, K. Koumoto, *J. Mater. Chem.* 13 (2003) 608–613.
- [46] D.M. Smith, A.R. Chughtai, *Colloid Surf. A* 105 (1995) 47–77.
- [47] A. Santamaría, F. Mondragón, A. Molina, N.D. Marsh, E.G. Eddings, A.F. Sarofim, *Combust. Flame* 146 (2006) 52–62.
- [48] Y. Ohko, Y. Nakamura, N. Negishi, S. Matsuzawa, K. Takeuchi, *J. Photochem. Photobiol. A* 205 (2009) 28–33.
- [49] T. Tatsuma, S. Tachibana, T. Miwa, D.A. Tryk, A. Fujishima, *J. Phys. Chem. B* 103 (1999) 8033–8035.
- [50] T. Tatsuma, S. Tachibana, A. Fujishima, *J. Phys. Chem. B* 105 (2001) 6987–6992.
- [51] K. Teramura, T. Tanaka, T. Funabiki, *Langmuir* 19 (2003) 1209–1214.
- [52] F. Nsib, N. Ayed, Y. Chevalier, *Prog. Org. Coat.* 55 (2006) 303–310.
- [53] J. Huang, *Adv. Polym. Technol.* 21 (2002) 299–313.
- [54] M.N. Tchoul, W.T. Ford, G. Lolli, D.E. Resasco, S. Arepalli, *Chem. Mater.* 19 (2007) 5765–5772.
- [55] J. Liu, A.G. Rinzler, H. Dai, J.H. Hafner, R.K. Bradley, P.J. Boul, A. Lu, T. Iverson, K. Shelimov, C.B. Huffman, F. Rodriguez-Macias, Y. Shon, T.R. Lee, D.T. Colbert, R.E. Smalley, *Science* 280 (1998) 1253–1256.
- [56] J. Zhang, H. Zou, Q. Qing, Y. Yang, Q. Li, Z. Liu, X. Guo, Z. Du, *J. Phys. Chem. B* 107 (2003) 3712–3718.